HHS Public Access

Author manuscript

Cancer Res. Author manuscript; available in PMC 2022 August 24.

Published in final edited form as:

Cancer Res. 2020 September 15; 80(18): 3855–3866. doi:10.1158/0008-5472.CAN-19-3713.

RAD51AP1 deficiency reduces tumor growth by targeting stem cell self-renewal

Allison E. Bridges[1,#], **Sabarish Ramachandran**[1,2,#], **Rajneesh Pathania**[1,3,#], **Utkarsh Parwal**[1], **Adrienne Lester**[4], **Pragya Rajpurohit**[1], **Daley S. Morera**[1], **Nikhil Patel**[5], **Nagendra Singh**[1,6], **Hasan Korkaya**[1,6], **Santhakumar Manicassamy**[1,6], **Puttur D. Prasad**[1,6], **Vinata B. Lokeshwar**[1,6], **Bal L. Lokeshwar**[1,6], **Vadivel Ganapathy**[1,2], **Muthusamy Thangaraju**[1,6,*]

[1]Department of Biochemistry and Molecular Biology, Augusta University, Augusta, GA 30912, USA

[2]Department of Cell Biology and Biochemistry, Texas Tech University Health Sciences Center, Lubbock, TX 79430, USA

[3]Epigenetics & Stem Cell Biology Laboratory, National Institute of Environmental Health Sciences, Research Triangle Park, NC 27709, USA.

[4]Depatment of Undergraduate Health Professions, College of Allied Health Sciences, Augusta University, Augusta, GA 30912, USA

[5]Department of Pathology, Augusta University, Augusta, GA 30912, USA

[6]Department of Georgia Cancer Center Medical College of Georgia, Augusta University, Augusta, GA 30912, USA

Abstract

RAD51AP1 (RAD51-associated protein 1) plays an integral role in homologous recombination (HR) by activating RAD51 recombinase. HR is essential for preserving genome integrity and RAD51AP1 is critical for D-loop formation, a key step in HR. Although RAD51AP1 is involved in maintaining genomic stability, recent studies have shown that RAD51AP1 expression is significantly upregulated in human cancers. However, the functional role of RAD51AP1 in tumor growth and the underlying molecular mechanism(s) by which RAD51AP1 regulates tumorigenesis have not been fully understood. Here we use Rad51ap1 knockout mice in genetically engineered mouse (GEM) models of breast cancer to unravel the role of RAD51AP1 in tumor growth and metastasis. RAD51AP1 gene transcript was increased in both luminal estrogen receptor-positive breast cancer (ER+BC) and basal triple-negative breast cancer (TNBC), which is associated with

[*]**Corresponding Author**. Muthusamy Thangaraju, PhD., Department of Biochemistry and Molecular Biology, Medical College of Georgia, Augusta University, 1410 Laney Walker Blvd., CN-1171, Augusta, GA 30912. Phone: 706-721-4219; Fax: 706-721-6608; mthangaraju@augusta.edu.

[#]Contributed equally.

Author contribution. A. E. B. and M. T. conceived the project, designed experiments, and wrote the manuscript; P. D. P., U. P., H. K., V. B. L., B. L. L., and V. G. helped on editorial input. S. R., P. R., U. P., and M. T. performed expression analysis, FACS, and animal experiments; R. P. and M. T. performed studies related to stem cells, mammospheres, and tumorospheres; S. R., S. M., P. D. P., and M. T. generated all mouse colonies and generated survival curve; A. E. B, A. L. and D. S. M. performed oncomine database analysis; N. G., N. P., S. M. helped histological and morphometric analyses; A. E. B. and M. T. performed data and compilation and analyses.

Conflict of Interest Statement. All authors declare no conflict of interest.

a poor prognosis. Conversely, knockdown of RAD51AP1 (RADP51AP1 KD) in breast cancer cell lines reduced tumor growth. Rad51ap1-deficient mice were protected from oncogene-driven spontaneous mouse mammary tumor growth and associated lung metastasis. In vivo, limiting dilution studies provided evidence that Rad51ap1 plays a critical role in breast cancer stem cell (BCSC) self-renewal. RAD51AP1 KD improved chemotherapy and radiation therapy response by inhibiting BCSC self-renewal and associated pluripotency. Overall, our study provides genetic and biochemical evidences that RAD51AP1 is critical for tumor growth and metastasis by increasing BCSC stem cell self-renewal and may serve as a novel target for chemotherapy- and radiation therapy-resistant breast cancer.

Introduction

Genome stability is dependent on the accurate repair of DNA double-strand breaks (DSBs). DSBs can arise either from exogenous sources like DNA damaging agents and ionizing radiation, or endogenous sources like reactive oxygen species (ROS), which are generated during either cellular metabolism or DNA replication (1). One major mechanism by which DSBs are repaired is by HR, which is essential for the preservation of genome integrity and maintenance of accurate genome duplication (2). HR utilizes the sister chromatid as a template and is considered a comparatively faithful DNA repair pathway. Defects in HR lead to destabilization of the genome and represent a progenitor of the tumor phenotype in mammals. In eukaryotic cells, HR reaction is mediated by RAD51 or DMC1 recombinases that are orthologous to bacterial RecA (3, 4). In response to DNA damage, RAD51 and other DNA repair proteins form nuclear foci, which are thought to represent the cellular structures responsible for DNA repair (5). Upon DNA damage induction by ionizing radiation (IR) or by treatment with interstrand DNA crosslinking agents, an increase in the number of RAD51 foci is observed (5). This provides evidence that RAD51 plays a critical role in the regulation of genomic integrity.

In recent years, a variety of recombinase partner proteins that enhance HR reaction by activating RAD51 or DMC1 have been identified (6). RAD51AP1 is one of such protein that has been shown to participate in the HR pathway (7, 8). Interaction of RAD51AP1, either with RAD51 or DMC1 recombinases, greatly enhances their recombinase activity and stimulates the D-loop formation (9), a key step for HR-mediated DNA repair in mitotic and meiotic cells. D-loop formation plays a critical role in mitochondrial DNA (mtDNA) function (10). In the past few years, somatic mtDNA mutations have been identified in several types of human cancers (11–13).

RAD51AP1 KD in human cells leads to increased levels of genomic instability and to decreased levels of homology-directed DNA repair (7, 8). Human cells with silenced *RAD51AP1* are viable, but are sensitized to the cytotoxic effects of interstrand cross-linking agents and ionizing radiation. However, human cells with depleted *RAD51AP1* are able to form RAD51 associated DNA damage foci with normal kinetics (7, 8), suggesting that RAD51AP1 is not essential for RAD51 associated foci formation. RAD51AP1 is also involved in growth- promoting signaling (14, 15), in which overexpression of *RAD51AP1* has been observed in cholangiocarcinoma (16), hepatocellular carcinomas (17), and acute

myeloid leukemia (18). However, the functional role of RAD51AP1 in tumor growth and the molecular mechanism(s) by which RAD51AP1 regulates tumorigenesis have not been clarified. In this study, we provide direct evidence that although RAD51AP1 plays an important role in maintaining genomic integrity in normal cells, the elevated levels of RAD51AP1 may be critical for early steps of neoplasia, where increased cell proliferation and replication stresses occur at higher than normal levels. Using *Rad51ap1* knockout mice, we provide genetic and biochemical evidences that RAD51AP1 is critical for tumor growth and metastasis using GEM models of breast cancer. We also provide evidence that the high expression of *RAD51AP1* in human cancers is correlated with a poor prognosis and, by increasing BCSC self-renewal, is associated with chemotherapy and radiation therapy resistance.

Materials and methods

Institutional compliance:

The animal experiments reported in this study were approved by the Augusta University (AU) Institutional Animal Care Use Committee (IACUC) and Biosafety Committees. Similarly, human breast cancer tissue and the surrounding normal tissues were obtained from the AU tumor bank as per the approval of the Institutional Review Board (IRB) and Human Assurance Committee.

Cell lines:

The primary human normal mammary epithelial cell line HMEC was obtained from the Lonza, Walkersville, MD. The human non-transformed normal mammary epithelial cell lines, MCF10A and MCF12A, were obtained from the American Type Culture Collection (ATCC) in June 2010. HBL100 was kindly provided by Dr. Saraswati Sukumar, Johns Hopkins University, Baltimore, MD in April 2003. ER^+BC cell lines (MCF7, T47D, ZR75.1, BT474, BT483, MDA-MB361, MDA-MB415), ER^-BC, and TNBC cell lines (MDA-MB231, MDA-MB468, and HCC1937), mouse non-transformed mammary epithelial cell line HC11, and mouse mammary tumor cell line 4T1 were obtained from ATCC between September 2008 and July 2011. The human breast cancer cell line, CAL51, was obtained from the DSMZ (Leibniz Institute DSMZ-German Collection of Microorganisms and Cell Cultures) in November 2011. The mouse mammary tumor cell line AT-3 was kindly provided by Dr. Estaban Celis, Georgia Cancer Center (GCC) at the AU in April 2014. AT-3 cell line was derived from an autologous mammary tumor cells originating in a MTAG (MMTV-PyMT/B6) transgenic mouse (19). Mammary tumors arising in MTAG mice closely mimic changes observed in human breast carcinomas over the course of the disease progression (20). AT-3 cell line is very useful to generate syngeneic transplant in C57BL/6 mouse and to study tumor physiology that is representative of typical disease states in humans. Cell lines from ATCC and DSMZ have been thoroughly tested and authenticated using morphology, karyotyping, and PCR based approaches to confirm the identity of the cell lines. The HMEC and MCF10A cells were grown in MEGM complete medium and MCF12A cells was grown in Dulbecco's modified Eagle's medium (DMEM)/F12 medium with 5% horse serum, 1% P/S, 20 ng/mL human epidermal growth factor (EGF), 100 ng/mL cholera toxin, 0.01 mg/mL bovine insulin and 500 ng/mL hydrocortisone. HBL100

cells were grown in McCoy 5A with 10% FBS. MCF7, BT20, HC11, and AT-3 cells were grown in DMEM medium with 10% FBS. T47D, ZR75.1, BT474, BT485, HCC1937, and 4T1 cells were grown in RPMI 1640 medium with 10% FBS. MDA-MB-231, −361, and MDA-MB-468 cells were grown in Leibovitz's L-15 medium with 10% FBS. MDA-MB415 cells was grown in Leibovitz's L-15 medium with 15% FBS, 1% P/S, and 0.01 mg/mL insulin. CAL51 cells were grown in DMEM medium supplemented with 20% fetal bovine serum (FBS), and 1% P/S. All these cell lines have been routinely tested for mycoplasma contamination using the Universal Mycoplasma Detection Kit obtained from ATCC (Manassas, VA), and the last mycoplasma test was performed in October 2019. Mycoplasma-free cell lines were used in all of our experiments.

Animals:

C57BL/6 (Stock # 000664), *MMTV-PyMT-Tg* (Stock # 002374), *MMTV-Neu-Tg* (Stock # 002376), *C3(1)-SV40-Tg* (Stock # 013591), and *Rad51ap1*-knockout [B6N(Cg)-*Rad51ap1*$^{tm1.1(KOMP)Vlcg/J}$, Stock # 025176) mice were obtained from the Jackson laboratories. All these mice were bred and maintained in AU Animal Facility in accordance with the guidelines of the IACUC. All euthanasia protocols have performed in accordance with the regulations and guidelines presented by IACUC and LAS of AU.

Mammary gland single-cell preparation:

Mammary gland single-cell preparation was carried out as described previously (15, 21). Briefly, the thoracic and inguinal mammary glands were dissected from mice. The tissues were digested for 6–8 h at 37°C in DMEM/F12 medium supplemented with 10% FBS and 1% P/S and 750 U/ml Collagenase and 250 U/ml hyaluronidase. After this step, the organoids were collected by centrifugation and then subjected to ACK treatment for red blood cell lysis followed by trypsin (0.5%) and dispase (5mg/ml) treatment separately. All reagents were obtained from STEMCELL Technology unless stated otherwise.

Analysis of mammary stem/progenitor (MaSC) and breast cancer stem cells (BCSCs):

For isolation of MaSC and BCSCs, we used CD24^{lo} and CD49f^{hi} as markers for normal MaSC and CD44/CD24 double-positive for human BCSCs and CD49f/CD24 double-positive for mouse BCSCs as described in our previous manuscripts (15, 21) and studies from other laboratories (22, 23). We used the following antibodies for this study: CD49f and CD24 (STEMCELL Technology and eBioscience), CD45, CD31, CD49f, CD44 (BD bioscience), and Ter119 and CD61 (eBioscience). Blocking was done for 10 min with rat serum. Cells were stained for 30 min on ice and washed with staining media. Finally, cells were resuspended in staining media containing 7-aminoactinomycin D (1 μg/ml) or 4'−6-diamidino-2-phenylindole (DAPI, 1 μg/ml) to stain dead cells. Cells were sorted through Mo flow cell sorter and flow cytometry data was analyzed using LSR II and Flow-jo as described before in our manuscripts (15, 21).

Immunoblot analysis:

For immunoblot (IB) analysis, cell lysates were prepared from cell lines and mammary tissues as described before (24, 25). Protein samples were fractionated on SDS-PAGE gels

and transferred to Protran nitrocellulose membrane (Whatman GmbH). Membranes were blocked with 5% non-fat dry milk and exposed to primary antibody at 4°C overnight followed by treatment with appropriate secondary antibody, conjugated to horseradish peroxidase at room temperature for 1 h, and developed by Enhanced Chemiluminescence Super Signal Western System and the signals captured on an x-ray film.

Methods for: **1**) generation of *RAD51AP1shRNA*-expressing stable cell lines; **2**) Clonogenic assays; **3**) generation of Paclitaxel-resistant cell lines; **4**) generation of *Rad51ap1*$^{-/-}$-*MMTV-PyMT*-Tg, *Rad51ap1*$^{-/-}$-*MMTV-Neu*-Tg, and *Rad51ap1*$^{-/-}$-*C3(1)-SV40*-Tg, mice; 5) *in vivo* limiting dilution assay; **6**) mouse genotyping; **7**) mouse xenograft; **8**) mouse syngeneic transplants; **9**) generation of mammospheres and tumorospheres; **10**) RNA isolation and PCR analysis; and **10**) Reverse transcriptase PCR are provided in the supplementary methods.

Statistical analysis:

Statistical analysis was done using 1-way ANOVA followed by Bonferroni multiple comparison test and also using student's t-test with two-tail distribution. The software used was Graph Pad Prism, version 8.0. A value of $p < 0.05$ was considered statistically significant. Kaplan-Meier analyses (http://kmplot.com/analysis/) were used to assay group differences in tumor-free survival. TCGA data base, UCGC genome, and DAVID (http://david.abcc.ncifcrf.gov) were also used to analyze RAD51AP1 expression. Graph Pad and Excel programs were used to draw figures.

Results

RAD51AP1 expression is upregulated in human breast cancer and is associated with a poor prognosis:

Oncomine database analysis (TCGA and GOBO) provides evidence that *RAD51AP1* (human) gene expression is increased in human breast cancer (15). To validate this observation, we analyzed *RAD51AP1* gene expression in human primary breast tumor tissues, which are ER^{+}BC and TNBC, with respective controls. Irrespective of hormone receptor status, *RAD51AP1* expression is significantly elevated in human breast cancer tissues when compared to normal tissues (Fig. 1A). Quantitative real-time PCR (qPCR) analysis provided evidence that *RAD51AP1* expression is significantly higher in human basal TNBC when compared to luminal ER^{+}BC (Fig. 1B). This observation was further confirmed by the TCGA database analysis (Fig. 1C). We then analyzed the functional correlation between *RAD51AP1* expression and the overall survival of breast cancer patients using Kaplan-Meier Plotter analysis. We found that high *RAD51AP1* expression is negatively associated with relapse-free survival (RFS) in both luminal ER^{+}BC and basal TNBC (Fig. 1D), distant metastasis-free survival (DMFS), and overall survival (Fig. S1A–B). We also analyzed RAD51AP1 expression in human normal immortalized mammary epithelial cell lines, luminal ER^{+}BC, and basal TNBC cell lines and recapitulated the similar findings, which were seen in human breast tumor tissues (Figs. 1E–F and S1C).

RAD51AP1 KD in human breast cancer cells reduces tumor growth:

As shown in Fig. 1, RAD51AP1 expression is amplified in human breast tumor tissues and cell lines. We then asked whether *RAD51AP1* KD in these cell lines would reduce tumor growth. *RAD51AP1* KD in CAL51, a TNBC cell line, was confirmed by expression analyses (Figs. 2A and S2A). *RAD51AP1* KD significantly reduced cell growth, which was measured by colony formation assays as described before (25, 26) (Fig. 2B). This observation was recapitulated in a mouse xenograft assay as describe before (24, 27). *RAD51AP1* KD significantly reduced tumor size and mass (Figs. 2C–E). Immunohistochemical (IHC) analysis reveals that *RAD51AP1* KD reduced tumor growth by inhibiting tumor cell proliferation assessed by Ki67 staining (Figs. 2F and S2B). These observations were also recapitulated in two more human breast cancer cell lines ZR75.1 (a human luminal ER+BC cell line) and MB231 (a human basal TNBC cell line) (Figs. S2C–J). Altogether, these results provide evidence that 1) RAD51AP1 expression is significantly elevated in human breast cancer tissues and cell lines; 2) This increased *RAD51AP1* expression is associated with reduced overall survival; 3) and *RAD51AP1* ablation leads to reduced tumor growth by inhibiting cell proliferation.

Rad51ap1 KD reduced tumor growth in syngeneic mouse models:

To confirm the prosurvival potential of RAD51AP1, we used mouse models of breast cancer. First, we analyzed Rad51ap1 (mouse) expression in normal immortalized mouse mammary epithelial cell line (HC11) and the mouse mammary tumor cell lines (AT-3 and 4T1). Rad51ap1 expression is significantly elevated in mouse mammary tumor cell lines when compared to a normal immortalized cell line (Figs. S3A–B). To determine the role of Rad51ap1 in mouse mammary tumor growth, we knocked down *Rad51ap1* in the AT-3 cell line and confirmed it by expression analyses (Figs. 3A and S3C). *Rad51ap1* ablation lead to reduced cell growth *in vitro* (Figs. 3B–C). This observation was recapitulated in an *in vivo* syngeneic mouse model. We subcutaneously implanted *pLKO.1* and *Rad51ap1shRN*A expressing AT-3 cells into the mammary fat pad of C57BL/6 mice and allowed them to grow for seven weeks. We measured tumor size and weight. *Rad51ap1* KD significantly reduced tumor size and weight (Fig. 3D–F). Histological sections provided evidence that *Rad51ap1* KD significantly reduced tumor growth by inhibiting tumor cell proliferation (Figs. 3G and S3D).

Rad51ap1 knockout mice confer resistance to tumor growth:

The biological role of RAD51AP1 in tumor growth and progression was further analyzed in wild-type ($Rad51ap1^{+/+}$) and *Rad51ap1* knockout ($Rad51ap1^{-/-}$) mice. *Rad51ap1* knockout was confirmed by genotyping and expression analysis (Figs. 4A and S4A–B). $Rad51ap1^{-/-}$ mice are normal, viable with no overt phenotype. To test the role of *Rad51ap1* in tumor growth and progression, we repeated the syngeneic transplant of AT-3 cells, which has functional Rad51ap1, into the mammary fat pad of $Rad51ap1^{+/+}$ and $Rad51ap1^{-/-}$ mice and monitored tumor growth for seven weeks. Although AT-3 tumor cells were able to elicit rapid tumorigenesis in $Rad51ap1^{+/+}$ mice, the tumor growth was significantly compromised in $Rad51ap1^{-/-}$ mice (Fig. 4B). The reduced tumor growth was also evidenced in tumor size and weight (Fig. 4C–D). Histological examination of tumor tissues revealed that

Rad51ap1 deletion reduced tumor growth by inhibiting tumor cell proliferation (Figs. 4E–F). Together, these data provide strong evidence that Rad51ap1 plays a critical role in the tumor microenvironment and that *Rad51ap1* deficiency produces a microenvironment which is not conducive for tumor cells to grow.

Rad51ap1 deficiency impedes tumor growth in spontaneous mammary tumorigenesis:

Based on the relative expression of RAD51P1 in normal and tumor tissues and cell lines, *RAD51AP1* overexpression has been reported in human cancers (15–18). Conversely, a recent study has reported the reduced *RAD51AP1* expression (due to the CpG methylation of *RAD51AP1* promoter) in prostate cancer cells (28). However, there is no direct evidence to show whether RAD51AP1 functions either as a tumor suppressor or a promoter of tumorigenesis. Hence, to test the relative contribution of RAD51AP1 in tumorigenesis, first, we analyzed the cell type-specific expression of *Rad51ap1* in the mammary epithelium. As shown in Fig. S5A, single-cell suspensions derived from the normal control mammary glands showed three distinct populations namely basal myoepithelial stem cells ($Lin^{-}CD49f^{hi}CD24^{lo}$), luminal progenitor ($Lin^{-}CD49f^{lo}CD24^{hi}$), and stromal ($Lin^{-}CD49f^{-}CD24^{-}$) cells. Using FACS sorter, we isolated these three different cell types separately and analyzed *Rad51ap1* gene expression. We found a relatively higher expression of *Rad51ap1* in basal myoepithelial stem cells compared to the luminal progenitor and stromal cells (Figs S5A–C). Analysis of *Rad51ap1* expression in normal and tumor tissues obtained from three-different spontaneous mouse mammary tumor models (*MMTV-PyMT-Tg*, *MMTV-Neu-Tg*, and *C3(1)-SV40-Tg*) revealed that *Rad51ap1* expression is significantly elevated in tumor tissues compared to normal (Fig. 5A–B). To determine the functional role of *Rad51ap1* in mammary tumorigenesis, we crossed $Rad51ap1^{-/-}$ mice with *MMTV-PyMT-Tg* (*PyMT-Tg*) and *MMTV-Neu-Tg* (*Neu-Tg*), both of which mimic human luminal progenitor (29, 30), and *C3(1)-SV40-Tg* (*C3(1)-Tg*) mice, which mimics human basal TNBC (31). Age-matched littermates of $Rad51ap1^{+/+}$ and $Rad51ap1^{-/-}$ in *PyMT-Tg*, *Neu-Tg*, and *C3(1)-Tg* background (n=25 in each), respectively, were allowed to form spontaneous tumors and monitored closely for signs of tumor development. Percentage of animals in which tumors developed, and time of tumor appearance in each genotype was monitored. Time until mouse sacrifice due to either the tumor burden or disease-free survival was also noted and used to calculate percent survival. After euthanizing the mice, total number of primary tumors formed in each genotype and lung metastatic nodules were also recorded. We found that there was no significant difference in the percent of tumor incidence between $Rad51ap1^{+/+}$-*PyMT-Tg* and $Rad51ap1^{-/-}$-*PyMT-Tg* mice as well as $Rad51ap1^{+/+}$-*C3(1)-Tg* and $Rad51ap1^{-/-}$-*C3(1)-Tg* mice (Figs. 5C and 5E). Irrespective of *Rad51ap1* genotypes, almost 100% of *Rad51ap1-PyMT-Tg* and *Rad51ap1-C3(1)-Tg* mice developed tumors. Although no significant difference was observed in tumor incidence between wild type and *Rad51ap1* knockout mice, the tumor latency was significantly longer with reduced number of lung nodules, which led to increased overall survival of *Rad51ap1* deficient mice when compared with the wild type littermates (Figs. 5C & E). However, significant differences were observed in the percent of tumor incidence, time of tumor formation, number of lung nodules, and overall survival between $Rad51ap1^{+/+}$-*Neu-Tg* and $Rad51ap1^{-/-}$-*Neu-Tg* mice (Fig. 5D). Altogether, these results provide strong and direct evidence that Rad51ap1 plays a critical role in mammary tumor growth and progression,

and that *Rad51ap1* deficiency significantly abrogated tumor formation with extended overall survival.

RAD51AP1 deficiency reduces cancer stem cell self-renewal signaling:

As shown in Figures 1–5, RAD51AP1 expression is amplified in human and mouse mammary tumors, and *RAD51AP1* deficiency has a significant impact on tumor growth and metastasis retardation. Therefore, we attempted to elucidate the molecular mechanism(s) by which *RAD51AP1* deficiency reduces tumor growth. We analyzed genes that are involved in epithelial cell differentiation, breast cancer stem cell (BCSC) formation, pluripotency, and EMT/metastasis using vector control (*pLKO.1*) and *RAD51AP1shRNA* transfected CAL51 cell line. *RAD51AP1* KD significantly increased the expression of epithelial differentiation marker *CDH1* (*E-cadherin*) with a significant reduction in BCSC markers (*CD44* and *CD49f*) and pluripotent stem cell markers (*NANOG* and *KLF4*) (Fig. 6A). These results were recapitulated in tumor tissues derived from the AT-3-*pLKO.1* and AT-3-*Rad51ap1shRNA* as well as *Rad51ap1*$^{-/-}$-*C3(1)-Tg* and *Rad51ap1*$^{-/-}$-*C3(1)-Tg* mice (Figs. 6B–C). These findings suggest that RAD51AP1 plays a critical role in BCSC self-renewal signaling.

These observations are supported by the previous studies in which *RAD51AP1* expression is positively associated with stem cell self-renewal (15), and stem cells are highly reliant on DNA repair mechanisms to maintain the pluripotency (32). Therefore, to provide more direct evidence for the role of RAD51AP1 in BCSC self-renewal, we analyzed BCSC populations in CAL51-*pLKO.1* and CAL51-*RAD51AP1shRNA* expressing cells. As shown in Fig. S5A, the normal mammary gland shows three distinct populations namely luminal ($Lin^-CD49f^{lo}CD24^{hi}$), basal ($Lin^-CD49f^{hi}CD24^{lo}$), and stromal ($Lin^-CD49f^-CD24^-$). However, we have recently shown that tumor tissues derived from the *MMTV-Neu-Tg* (15, 21) and *MMTV-Hras-Tg* (24) mice showed only two distinct populations: ($Lin^-CD49f^+CD24^+$), tumorigenic, and ($Lin^-CD49f^-CD24^-$), non-tumorigenic. As described before by Al-Hajj *et al* (22), we used CD44 and CD24 as cell surface markers for human and CD49f and CD24 for mouse (15, 21). Analysis of CAL51-*pLKO.1* shows only two distinct populations ($CD44^{hi/(+)}$ $CD24^{hi/(+)}$) and ($CD44^{lo/(-)}$ $CD24^{lo/(-)}$) (Fig. 6D). Thus, we used CD44 and CD24 double-positive cells as a human BCSCs and CD49f and CD24 double-positive cells as a mouse BCSCs as described before (15, 21). We found that *RAD51AP1* KD significantly reduced the BCSC pool ($CD44^+CD24^+$) when compared to control vector-transfected cells (Figs. 6D–E). We sorted the BCSCs ($CD44^+CD24^+$) by FACS and generated tumorospheres using stem cell enrichment medium as described before (15, 21). *RAD51AP1* KD significantly reduced the size and number of tumorospheres (primary, secondary, and tertiary) when compared with *pLKO.1* expressing CAL51 cells (Figs S6A–B). These observations were recapitulated in tumor tissues derived from the syngeneic transplant of AT-3-*pLKO.1* and AT-3-*Rad51ap1shRNA* (Figs. S6C–F). We also analyzed the BCSC populations in tumor tissues obtained from *Rad51ap1*$^{+/+}$-*C3(1)-Tg* and *Rad51ap1*$^{-/-}$-*C3(1)-Tg* mice. We found that *Rad51ap1* deficiency not only reduced the BCSC pool, but also reprogramed BSCS (Figs. 6F–G) and reduced the size and number of tumorospheres (primary, secondary, and tertiary) (Figs. 6H–I). To test the role of Rad51ap1 in BCSC self-renewal further, we performed the limiting dilution of FACS sorted

CD49f^{+}CD24^{+} double-positive (BCSCs) and CD49f^{-}CD24^{-} double-negative (non-stem) cells from the tumor tissues derived from *Rad51ap1*$^{+/+}$-*MMTV-Neu-Tg* and *Rad51ap1*$^{-/-}$-*MMTV-Neu-Tg* mice. First, we analyzed Rad51ap1 expression in BCSCs and non-stem cells and found that significantly increased *Rad51ap1* expression (>28-fold) in BCSCs than the non-stem cells (Fig. S6G). Then, we injected BCSCs and non-stem cells (from 1×10^{1} to 1×10^{6} cells) in the mammary fat pad of NOD/SCID mice. *Rad51ap1* deficiency significantly reduced the tumor forming potential of CD49f^{+}CD24^{+} double-positive cells while CD49f^{-}CD24^{-} double-negative cells were unable to form tumors even in 1×10^{6} cells. (Fig. S6H) These results demonstrate the importance of RAD51AP1 in stem self-renewal and gene expression that are involved in stem cell self-renewal.

RAD51AP1 deficiency potentiates chemotherapy and radiation therapy response by inhibiting stem cell self-renewal signaling:

As shown in Fig. 6, RAD51AP1 plays a critical role in BCSC self-renewal and *RAD51AP1* deficiency not only reduced the BCSC pool but also reprogramed BCSCs (three distinct population as seen in normal control mammary gland). Since, cancer stem cells (CSC) have been implicated in conventional chemotherapy and radiation therapy resistance (33), we explored the clinical utility of *RAD51AP1* KD in inducing sensitivity to chemo- and radiation- therapy. CSCs are a small population of cells (1–2%) with unique characteristics such as self-renewal, high proliferation rate, and the ability to generate heterogenic lineages of cancer cells (22, 23). Therefore, there are various types of CSCs within a tumor, with different mutational profiles and in different stages of cell cycling. Typically, within a tumor, there is one dominant population driving tumor progression, but there are always other minor populations waiting for an opportunity to expand. This opportunity often comes when the dominant CSC population is destroyed during chemotherapy or ionizing radiation. The smaller CSC population, that was either in a quiescent state during treatment, or has acquired resistance to therapeutics, can emerge and promote new tumor growth. The recurring tumor is often more aggressive and resistant to previous therapeutics, thereby increasing the risk for metastasis and requiring a new treatment strategy to be devised. As shown in Fig. 6, RAD51AP1 appears to play an important role in CSC maintenance and self-renewal and, thus, we asked whether *RAD51AP1* deficiency will potentiate chemotherapy (Paclitaxel, PTX) and radiation therapy (ionizing radiation, IR) response in cancer cells. *RAD51AP1* KD (*RAD51AP1shRNA*) in human breast cancer cell line (CAL51) and mouse mammary tumor cell line (AT-3) significantly potentiated both PTX and IR-induced apoptosis when compared to vector-transfected cells (Figs. 7A–B). To provide more concrete evidence for the role of RAD51AP1 in drug resistance, we isolated mammary epithelial cells from the tumor tissues obtained from *Rad51ap1*$^{+/+}$-*C3(1)-Tg* and *Rad51ap1*$^{-/-}$-*C3(1)-Tg* mice and then treated with PTX and IR. We found that *Rad51ap1* deficiency potentiates PTX and IR response by increasing apoptotic cell death (Fig. 7C). These data demonstrate that *RAD51AP1* deficiency indeed leads to increased cellular sensitivity to chemotherapy and radiation. We then asked whether PTX resistance is associated with increased RAD51AP1 expression and if *RAD51AP1* KD would resensitize the CAL51 cells to chemotherapy response. Thus, we generated PTX resistant CAL51 cell line by increasing PTX concentration (10–250 nM) as described before (34). We analyzed RAD51AP1 expression in PTX-sensitive (PTX-S) and PTX-resistant (PTX-R) cell lines

and found that RAD51AP1 expression is significantly increased in PTX-R cells compared to PTX-S cells (Fig. 7D). Then we took the CAL51-PTX-R cell line and infected with *pLKO.1* and *RAD51AP1shRNA*. *RAD51AP1* KD was confirmed by qPCR analysis (Fig. 7E). We found that *RAD51AP1* depletion re-sensitizes CAL51-PTX-R cells for PTX as evidenced by increased apoptotic cell death (Fig. 7F). We also found that *RAD51AP1* deficiency is associated with a reduced BCSC pool (Figs. 7G–H). We next analyzed the expression of stem cell self-renewal genes like *NANOG*, *KLF4*, *SOX2* and *OCT4* and found that *RAD51AP1* KD in PTX-R cells significantly reduced *NANOG* and *KLF4* expression (Figure 7I). These data provide direct evidence that RAD51AP1 plays a critical role in resistance to chemotherapy and radiation therapy in that RAD51AP1 deficiency not only potentiates chemotherapy response, but also resensitizes the resistant cancer cells to chemotherapy. Overall, our results provide evidence that RAD51AP1 plays a critical role in breast cancer growth and metastasis by regulating BCSC self-renewal, which involved in tumor growth and metastasis, drug resistance, and reduced overall survival. Thus, RAD51AP1 is an attractive target for the prevention and treatment of breast cancer.

Discussion

In this study, we provide direct evidence that RAD51AP1 plays a critical role in tumor growth and chemotherapy resistance by regulating cancer stem cell (CSC) self-renewal and that *Rad51ap1* deficiency abrogates tumor growth and re-sensitizes cancer cells for chemotherapy by inhibiting CSC self-renewal signaling. Although RAD51AP1 plays a central role in HR and genome integrity, it also plays an important role in growth by promoting signaling in the early stages of tumor growth where replication stress occurs at higher than normal levels. Previous studies have shown increased expression of *RAD51AP1* in human tumor tissues (15–18), which can shift the balance from a pre-cancerous milieu to cancerous one. There was, however, no direct evidence that RAD51AP1 is directly involved in tumor growth and CSC self-renewal. Our investigation, for the first time, uncovered direct evidence showing that *RAD51AP1* expression is increased in different breast cancer subtypes and is inversely associated with overall survival. Furthermore, *Rad51ap1* deficiency in mice abrogated tumor growth and metastasis in GEM mouse models of breast cancer. However, *Rad51ap1* depletion did not affect the normal epithelial homeostasis in the mammary gland suggesting that Rad51ap1 is dispensable for normal growth. Therefore, functional inactivation of RAD51AP1 would have far-reaching implications in cancer prevention and treatment without affecting normal cells. Given the overexpression of *RAD51AP1* in breast cancer patients, especially in TNBC, RAD51AP1 could be explored as a potential biomarker for this breast cancer subtype.

Further, we found a significant discrepancy between results obtained from the *RAD51AP1* KD in human breast cancer cell line (CAL51)-driven mouse xenograft, mouse mammary tumor cell line (AT-3)-driven syngeneic transplant, and *Rad51ap1* knockout-driven spontaneous mammary tumor models. *RAD51AP1* KD is associated with a significant reduction in tumor growth (tumor size and volume) and cell proliferation (Ki67 staining) while *Rad51ap1* knockout has significant impact on inhibiting tumor metastasis rather than reducing primary tumor formation. This discrepancy mainly due to the less metastatic potential of CAL51 and AT-3 cell lines that are very occasionally metastasize to the lung.

Thus, we could not see the metastatic phenotype and unable to study the role of RAD51AP1 in tumor metastasis in these mouse models. However, GEM models, especially *PyMT-Tg* and *C3(1)-Tg*, tumors develop very aggressively within a very short period of time (2–5 months) and multiple signaling pathway(s) are involved in tumor development in these GEM models. Although there is no significant difference in the overall tumor incidence between wild type and *Rad51ap1* deficient mice, the time of tumor formation, number of tumors developed, and percent of lung metastasis are significantly reduced with increased overall survival in *Rad51ap1* knockout mice when compared to the wild type mice (Figs. 5C & E). However, we could see a clear decrease in the percent of tumor incidence, tumor growth, time of tumor formation, percent of lung metastasis and overall survival between *Rad51ap1* replete (+/+) and knockout (−/−) mice in *Neu-Tg* model (Fig. 5D). Therefore, *RAD51AP1* plays significant role in both breast tumor growth and metastasis, but slightly differs depending on the animal model used to study.

Our study provides mechanistic evidence that RAD51AP1 deficiency associated reduction in tumor growth and metastasis can be attributed to targeting signaling pathways that are involved in BCSCs self-renewal and maintenance. Although RAD51AP1 plays a critical role in HR and genomic stability, our study for the first time, provides evidence that RAD51AP1 also plays a critical role in BCSC self-renewal by targeting genes that are involved in BCSC self-renewal and pluripotency. We have shown that *RAD51AP1* expression is significantly increased in BCSCs than non-BCSCs (Fig. S5). We have also shown that *RAD51AP1* KD in human breast cancer cell lines and *Rad51ap1* deletion in GEM mouse models shows significantly reduced BCSC self-renewal, as evidenced by the reduction in tumorospheres size and number (primary, secondary, and tertiary) and reduction in the expression of self-renewal and pluripotent stem cell markers, which are the commonly and routinely used functional assays for the BCSC self-renewal (Fig. 6). In our previous study, we isolated BCSCs (CD49f and CD24 double-positive) and non-stem cells (CD49f and CD24 double-negative) and analyzed tumor-forming potential of these cells by serial dilution and found that only CD49f and CD24 double-positive cells were able to form tumors but not CD49f and CD24 double-negative cells (15, 21). However, in the current study, we are unable to provide direct evidence whether RAD51AP1 deficiency associated-tumor growth retardation is associated only with BCSCs not with non-stem cell population. A definitive answer to this question would require *in vivo* serial dilution-based tumor initiation experiments using BCSCs isolated from wild type and *Rad51ap1* knockout mice which are beyond the scope of this manuscript. Further, a recent study has shown that RAD51AP1 plays a critical role in lengthening of telomeres (35). Although human somatic cells lack telomerase activity, somatic stem and progenitor cells express detectable levels of telomerase, which contribute to the prolonged proliferative capacity of these cells. Thus, it is possible that the observed phenotypic changes in *Rad51ap1* deficient mice might also be associated with other signaling pathways, such as regulating telomere lengthening.

CSCs are believed to initiate and propagate tumorigenesis and are responsible for chemotherapy and radiation therapy resistance, metastasis, and tumor recurrence (35–38). With chemotherapeutic drugs targeting only the bulk of the cancer cells, but not CSC, the survival of CSCs reinitiates tumor formation in about 20–45% of patients within years or decades after treatment. This is a key challenge for clinicians who are trying to treat

patients and palliate the cancer to extend overall patient survival. Targeting CSCs is an attractive and potential strategy for cancer prevention and treatment. CSCs retain higher levels of DNA damage repair than normal healthy cells. Due to their high frequency of replication, understanding the mechanisms that promote successful repair and clearance of DNA strand breaks will allow us to determine the best way to undermine the system to either make cells more sensitive to conventional therapies or force them into apoptosis on their own. In this study, we have demonstrated the importance of RAD51AP1 in stem cell maintenance and also provided sufficient evidence showing that *RAD51AP1* deficiency has a profound impact on stem cell self-renewal by inhibiting genes involved in pluripotency (*NANOG*, *KLF4*, *OCT4*, and *SOX2*). Among these, NANOG, a transcription factor, serve as the master regulator of stem cell self-renewal (39). Similarly, OCT4, another transcription factor, has been shown to play a similar role in lung CSC (40). *OCT4* KD decreased lung CSC self-renewal and increased chemosensitivity in lung cancer model (41). Thus, reduced expression of *NANOG* and *OCT4* in *RAD51AP1* KD cells and *Rad51ap1* deficient mice could provide possible explanations for the reduced self-renewal, tumor growth, and metastasis in *Rad51ap1* deficient mouse models of breast cancer. RAD51AP1 should be seen as a novel target for cancer treatment that is applicable to a wide variety of cancer subtypes.

One of the important and significant findings of this study is that *Rad51ap1* deficiency significantly reduced tumor metastasis in GEM mouse models of breast cancer (Fig. 5). Tumor metastasis is associated with profound changes in the cell adhesion, polarity, and migratory properties of tumor cell and is collectively known as an epithelial mesenchymal transition (EMT). Loss of functional E-cadherin (*CHD1*) is an essential event for the EMT and is considered as a hallmark of the process (42). Interestingly, *RAD51AP1* KD in human breast cancer cell lines and *Rad51ap1* deficiency in GEM mouse models of breast cancer significantly rescued the *CHD1* expression. Further, the EMT markers *SNAI*1 (Snail) and *SNAI2* (Slug) have been associated with repression of E-Cadherin and also activation of local and distant metastasis, tumor recurrence, and poor prognosis (43, 44). The reduced expression of *SNAI*1 and *SNAI*2 observed in *RAD51AP1* KD breast cancer cells and *Rad51ap1* deficient mice provided further evidence for the reduced tumor metastasis observed in *Rad51ap*$^{-/-}$*-PyMT-Tg*, *Rad51ap*$^{-/-}$*-Neu-Tg*, and *Rad51ap*$^{-/-}$*-C3(1)-Tg* mice (Fig. 5). In addition, the reduced expression of Vimentin (*VIM*), which is selectively expressed in aggressive breast cancer cells (45), in *RAD51AP1* KD cells provide further evidence for the reduced metastasis observed in Rad51ap1 deficient cells. However, the molecular mechanism(s) by which RAD51AP1 regulates the EMT and associated tumor metastasis is not known and a separate study is warranted to provide more mechanistic evidence to explore the role of RAD51AP1 in the regulation of EMT and associated tumor metastasis.

Finally, our study clearly demonstrates that RAD51AP1 plays an important role in chemotherapy and radiation therapy resistance, and that functional inactivation of this gene can resensitize tumor cells to chemotherapy and radiation therapy response. Many cancer drugs produce DNA lesions at replication fork, and cancer cells utilize RAD51AP1 and other HR proteins to repair DSBs to maintain the cellular integrity. It has been shown that a cell's ability to repair DSBs significantly affects the outcome of cancer treatment;

cells deficient in HR and DNA damage repair process are hypersensitive to drug-induced cell death, resulting in a better chemotherapeutic response and outcome. Although the role of RAD51AP1 in the repair of various types of DNA damages has not been fully deciphered yet, we know for sure that its function is critical for HR-mediated repair of DNA strand breaks. We, therefore, believe that RAD51AP1 function imparts sensitivity to most, if not all, chemotherapeutic drugs that induce DNA strand breaks. Therefore, the increased sensitivity of chemotherapy and radiation therapy response in *RAD51AP1* KD cells could be associated to compromise in DNA damage repair function. This effect is not unique for human breast cancer cells and we have observed a similar effect with 5-Flurouracil (5-FU) resistant human colon cancer cells too. The connection between DNA repair and CSCs in chemotherapy and radiation therapy resistance was first established in high-grade primary brain tumors. The $CD133^+$ glioblastoma stem cells activate ATM and CHK1 more promptly than the $CD133^-$ cells. This molecular response enabled $CD133^+$ cells to survive during ionizing radiation, while $CD133^-$ population underwent cell death (46). Interestingly, subsequent studies have shown that there are significant increases in the expression of DNA repair genes in pancreatic, prostate, colon, and lung CSCs when exposed to standard chemotherapeutic agents and radiation therapy (47–49). Similarly, enhanced DNA repair ability has been described in BCSCs (48). BCSCs exhibit higher level of DNA repair genes (BRCA1, RAD51, ATM, ATR, and, CHK1) when compared to differentiated tumor cells (50). Along with the DNA repair potential of RAD51AP1, it also regulates CSC self-renewal. This is, in turn, involved in chemotherapy and radiation therapy response. Altogether, our study provides direct evidence that RAD51AP1 could become a novel target for cancer prevention and treatment and overcoming drug resistance.

Supplementary Material

Refer to Web version on PubMed Central for supplementary material.

Acknowledgments.

We thank Penny P. Roon, Donna Kumiski, and Dr. Brendan Marshall, in the Electron Microscopy and Histology core facility, Augusta University Cancer Center, for their help in histological analysis. This work was supported by Augusta University Intramural PSRP Pilot Award (IGPP00004), Start-up, and Bridge funding (MT).

References

1. Shrivastav M, De Haro LP, Nickoloff JA. Regulation of DNA double-strand break repair pathway choice. Cell Res 2008; 18: 134–147. [PubMed: 18157161]
2. Hoeijmakers JH. Genome maintenance mechanisms for preventing cancer. Nature 2001; 411: 366–374. [PubMed: 11357144]
3. Neale MJ, Keeney S. Clarifying the mechanics of DNA strand exchange in meiotic recombination. Nature 2006; 442: 153–158. [PubMed: 16838012]
4. Bishop DK, Park D, Xu L, Kleckner N. DMC1: A meiosis-specific yeast homolog of E. coli recA required for recombination, synaptonemal complex formation, and cell cycle progression. Cell 1992; 69: 439–456. [PubMed: 1581960]
5. Haaf T, Golub EI, Reddy G, Radding CM, Ward DC. Nuclear foci of mammalian Rad51 recombination protein in somatic cells after DNA damage and its localization in synaptonemal complexes. Proc Natl Acad Sci USA 1995; 92: 2298–2302. [PubMed: 7892263]

6. San Filippo J, Sung P, Klein H. Mechanism of eukaryotic homologous recombination. Annu Rev Biochem 2008; 77: 229–257. [PubMed: 18275380]
7. Modesti M, Budzowska M, Baldeyron C, Demmers JAA, Ghirlando R, Kannar R. RAD51AP1 is a structure-specific DNA binding protein that stimulates joint molecule formation during RAD51-mediated homologous recombination. Mol Cell 2007: 28: 468–481. [PubMed: 17996710]
8. Dray E, Dunlop MH, Kauppi L, Filippo JS, Wiese C, Tsai M-S, et al. Molecular basis for enhancement of the meiotic DMC1 recombinase by RAD51 associated protein 1 (RAD51AP1). Proc Natl Acad Sci USA 2011; 108: 3560–3565. [PubMed: 21307306]
9. Wiese C, Dray E, Groesser T, Filippo JS, Shi I, Collins DW, et al. Promotion of homologous recombination and genomic stability by RAD51AP1 via RAD51 recombinase enhancement. Mol Cell 2007; 28: 482–490. [PubMed: 17996711]
10. Lièvre A, Blons H, Houllier AM, Laccourreye O, Brasnu D, Beaune P, et al. Clinicopathological significance of mitochondrial D-Loop mutations in head and neck carcinoma. Br J Cancer 2006; 94: 692–697. [PubMed: 16495928]
11. Polyak K, Li Y, Zhu H, Lengauer C, Willson JK, Markowitz SD, et al. Somatic mutations of the mitochondrial genome in human colorectal tumours. Nat Genet 1998; 20: 291–293. [PubMed: 9806551]
12. Fliss MS, Usadel H, Caballero OL, Wu L, Buta MR, Eleff SM, et al. Facile detection of mitochondrial DNA mutations in tumors and bodily fluids. Science 2000; 287: 2017–2019. [PubMed: 10720328]
13. Richard SM, Bailliet G, Paez GL, Bianchi MS, Peltomaki P, Bianchi NO. Nuclear and mitochondrial genome instability in human breast cancer. Cancer Res 2000; 60: 4231–4237. [PubMed: 10945635]
14. Parplys AC, Kratz K, Speed MC, Leung SG, Schild D, Wiese C. RAD51AP1-deficiency in vertebrate cells impairs DNA replication. DNA Repair (Amst) 2014; 24: 87–97. [PubMed: 25288561]
15. Pathania R, Ramachandran S, Mariappan G, Thakur P, Shi H, Chi J-H, et al. Combined inhibition of DNMT and HDAC blocks the tumorigenicity of cancer stem-like cells and attenuates mammary tumor growth. Cancer Res 2016; 76: 3224–3235. [PubMed: 27197203]
16. Obama K, Satoh S, Hamamoto R, Sakai Y, Nakamura Y, Furukwa Y. Enhanced expression of RAD51 associating protein-1 is involved in the growth of intrahepatic cholangiocarcinoma cells. Clin Cancer Res 2008; 14: 1333–1339. [PubMed: 18316552]
17. Song LJ, Zhang WJ, Chang ZW, Pan YF, Zong H, Fan QX, et al. PU.1 is identified as a novel metastasis suppressor in hepatocellular carcinoma regulating the miR-615–5p/IGF2 axis. Asian Pac J Cancer Prev 2015; 16: 3667–3671. [PubMed: 25987019]
18. Schoch C, Kern W, Kohlmann A, Hiddemann W, Schnittger S, Haferlach T. Acute myeloid leukemia with a complex aberrant karyotype is a distinct biological entity characterized by genomic imbalances and a specific gene expression profile. Genes Chromosomes Cancer 2005; 43: 227–238. [PubMed: 15846790]
19. Stewart TJ, Abrams SI. Altered immune function during long-term host-tumor interactions can be modulated to retard autochthonous neoplastic growth. J Immunol 2007; 179: 2851–2859. [PubMed: 17709499]
20. Lin EY, Jones JG, Li P, Zhu L, Whitney KD, Muller WJ, et al. Progression to malignancy in the polyoma middle T oncoprotein mouse breast cancer model provides a reliable model for human diseases. Am J Pathol 2003; 163: 2113–2126. [PubMed: 14578209]
21. Pathania R, Ramachandran S, Elangovan S, Padia R, Yang P, Cingu S, et al. DNMT1 is essential for mammary and cancer stem cell maintenance and tumorigenesis. Nat Commun 2015; 6: 6910. [PubMed: 25908435]
22. Al-Hajj M, Wicha MS, Benito-Hernandez A, Morrison SJ, Clarke MF. Prospective identification of tumorigenic breast cancer cells. Proc Natl Acad Sci USA 2003; 100: 3983–3988. [PubMed: 12629218]
23. Lawson DA, Bhakta NR, Kessenbrock K, Prummel KD, Yu Y, Takai K, et al. Single-cell analysis reveals a stem-cell program in human metastatic breast cancer cells. Nature 2015; 526: 131–135. [PubMed: 26416748]

24. Elangovan S, Pathania R, Ramachandran S, Ananth S, Padia RN, Srinivas SR, et al. Molecular mechanism of SLC5A8 inactivation in breast cancer. Mol Cell Biol 2013; 33: 3920–3935. [PubMed: 23918800]
25. Elangovan S, Ramachandran S, Venkatesan N, Ananth S, Gnana-Prakasam JP, Martin PM, et al. SIRT1 is essential for oncogenic signaling by estrogen/estrogen receptor α in breast cancer. Cancer Res 2011; 72: 6654–6664.
26. Thangaraju M, Gopal E, Martin PM, Ananth S, Smith SB, Prasad PD, et al. SLC5A8 triggers tumor cell apoptosis through pyruvate-dependent inhibition of histone deacetylases. Cancer Res 2006; 66: 11560–11564. [PubMed: 17178845]
27. Elangovan S, Pathania R, Ramachandran S, Ananth S, Padia RN, Lan L, et al. The niacin/butyrate receptor GPR109A suppresses mammary tumorigenesis by inhibiting cell survival. Cancer Res 2014; 74: 1166–78. [PubMed: 24371223]
28. Wang Y, Yu Q, Cho AH, Rondeau G, Welsh J, Adamson E, et al. Survey of differentially methylated promoters in prostate cancer cell lines. Neoplasia 2005; 7: 748–760. [PubMed: 16207477]
29. Li Y, Welm B, Podsypanina K, Huang S, Chamorro M, Zhang X, et al. Evidence that transgenes encoding components of the Wnt signaling pathway preferentially induce mammary cancers from progenitor cells. Proc Natl Acad Sci USA 2003; 100: 15853–15858. [PubMed: 14668450]
30. Guy CT, Webster MA, Schaller M, Parsons TJ, Cardiff RD, Muller WJ. Expression of the neu protooncogene in the mammary epithelium of transgenic mice induces metastatic disease. Proc Natl Acad Sci USA 1992; 89: 10578–10582. [PubMed: 1359541]
31. Maroulakou IG, Anver M, Garrett L, Green JE. Prostate and mammary adenocarcinoma in transgenic mice carrying a rat C3(1) simian virus 40 large tumor antigen fusion gene. Proc Natl Acad Sci USA 1994; 91: 11236–11240. [PubMed: 7972041]
32. O'Brien CA, Kreso A, Jamieson CH. Cancer stem cells and self-renewal. Clin Cancer Res 2010; 16: 3113–3120. [PubMed: 20530701]
33. Carnero A, Garcia-Mayea Y, Mir C, Lorente J, Rubio IT, LLenonart ME. The cancer stem-cell signaling network and resistance to therapy. Cancer Treat Rev 2016; 49: 25–36. [PubMed: 27434881]
34. Godwin AK, Meister A, O'Dwyer PJ, Huang CS, Hamilton TC, Anderson ME. High resistance to cisplatin in human ovarian cancer cell lines is associated with marked increase of glutathione synthesis. Proc Natl Acad Sci USA 1992; 89: 3070–3074. [PubMed: 1348364]
35. Barroso-González J, Garcia-Exposito L, Hoang SM, Lynskey ML, Roncaioli JL, Ghosh A, et al. RAD51AP1 Is an Essential Mediator of Alternative Lengthening of Telomeres. Mol Cell 2019; 76: 11–26.
[PubMed: 31400850]
36. Velasco-Velázquez MA, Popov VM, Lisanti MP, Pestell RG. The role of breast cancer stem cells in metastasis and therapeutic
implications. Am J Pathol 2011; 179: 2–11.
[PubMed: 21640330]
37. Morrison BJ, Schmidt CS, Lakhani SR, Reynolds BA, Lopez JA. Breast cancer stem cells: implications for therapy of breast cancer. Breast Cancer Res 2008; 10: 210. [PubMed: 18671830]
38. Yamashina T, Baghdadi M, Yoneda A, Kinsoshita I, Suzu S, Dosaka-Akita H, et al. Cancer stem-like cells derived from chemoresistant tumors have a unique capacity to prime tumorigenic myeloid cells. Cancer Res 2014; 74: 2698–2709. [PubMed: 24638980]
39. Gawlik-Rzemieniewska N, Bednarek I, The role of NANOG transcriptional factor in the development of malignant phenotype of cancer cells. Cancer Biol Ther 2016; 17, 1–10. [PubMed: 26618281]
40. Chen YC, Hsu HS, Chen YW, Tsai TH, How CK, Wang CY, et al. Oct-4 expression-maintained cancer stem-like properties in lung cancer-derived CD133-positive cells. PLoS One 2008; 3: e2637.
41. Hu T, Liu S, Breiter DR, Wang FW, Sun S. Octamer 4 small interfering RNA results in cancer stem cell-like cell apoptosis. Cancer Res 2008; 68: 6533–6540. [PubMed: 18701476]

42. Thiery JP, Sleeman JP. Complex networks orchestrate epithelial-mesenchymal transition. Nat Rev Mol Cell Biol 2006; 7: 131–142. [PubMed: 16493418]

43. Cheng CW, Wu PE, Yu JC, Huang CS, Yue CT, Wu CW, et al. Mechanisms of inactivation of E-cadherin in breast carcinoma: modification of the two-hit hypothesis of tumor suppressor gene. Oncogene 2001; 20: 3814–3823. [PubMed: 11439345]

44. Come C, Magnino F, Bibeau F, Santa Barbara PD, Becker KF, Theillet C, et al. Snail and slug play distinct roles during breast carcinoma progression. Clin Cancer Res 2006; 12: 5395–5402. [PubMed: 17000672]

45. Hendrix MJ, Seftor EA, Seftor RE, Trevor KT. Experimental co-expression of vimentin and keratin intermediate filaments in human breast cancer cells results in phenotypic interconversion and increased invasive behavior. Am J Pathol 1997; 150: 483–495. [PubMed: 9033265]

46. Bao S, Wu Q, McLendon RE, Hao Y, Shi Q, Hielmeland AB, et al. Glioma stem cells promote radioresistance by preferential activation of the DNA damage response. Nature 2006; 444: 756–760. [PubMed: 17051156]

47. Mathews LA, Cabarcas SM, Hurt EM, Zhang X, Jaffee EM, Farrar WL. Increased expression of DNA repair genes in invasive human pancreatic cancer cells. Pancreas 2011; 40: 730–739. [PubMed: 21633318]

48. Gallmeier E, Hermann PC, Muller MT, Machado JG, Ziesch A, De Toni EN, et al. Inhibition of ataxia telangiectasia- and Rad3-related function abrogates the in vitro and in vivo tumorigenicity of human colon cancer cells through depletion of the CD133(+) tumor-initiating cell fraction. Stem Cells 2011; 29: 418–429. [PubMed: 21308861]

49. Bartucci M, Svernsson S, Romania P, Dattilo R, Patrizii M, Signore M, et al. Therapeutic targeting of Chk1 in NSCLC stem cells during chemotherapy. Cell Death Differ 2011; 19: 768–778. [PubMed: 22117197]

50. Zhang M, Behbod F, Atkinson RL, Landis MD, Kittrell F, Edwards D, et al. Identification of tumor-initiating cells in a p53-nullmouse model of breast cancer. Cancer Res 2008; 68: 4674–4682. [PubMed: 18559513]

Significance:

This study provides in vivo evidence that RAD51AP1 plays a critical role in breast cancer growth and metastasis by regulating BCSC self-renewal.

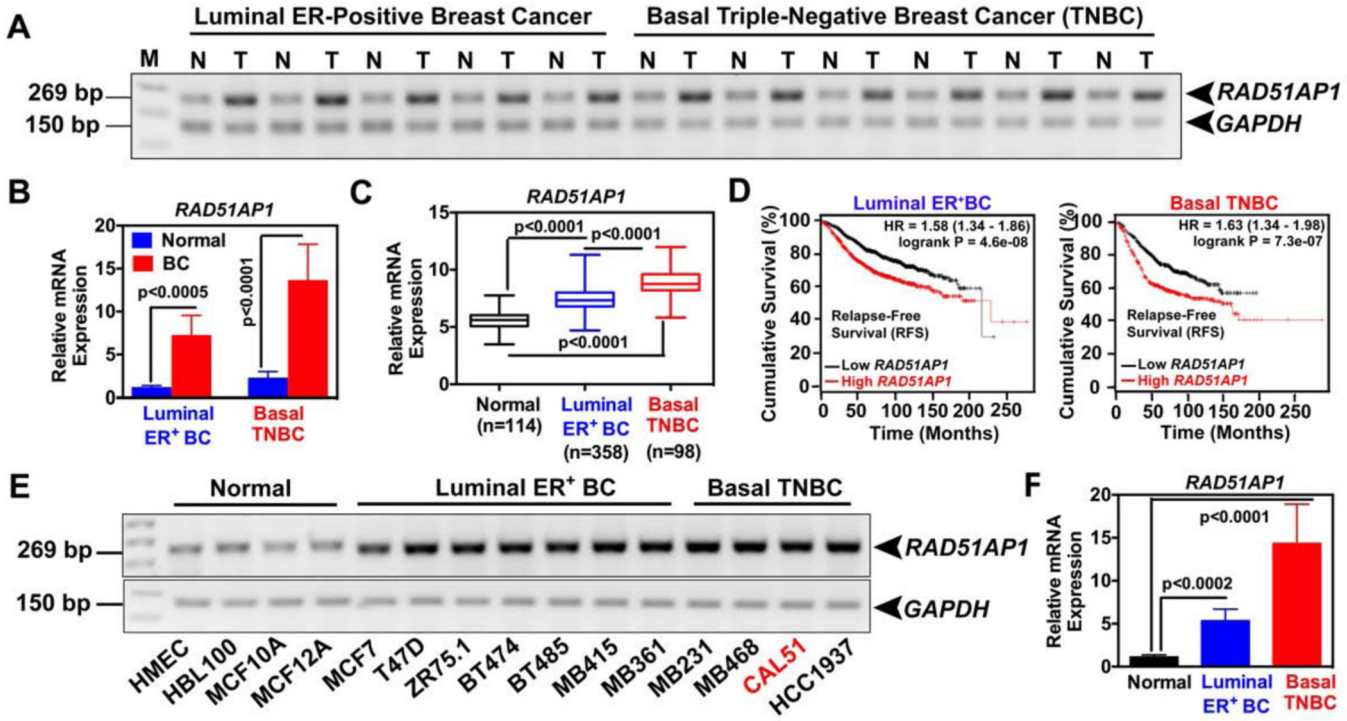

Figure 1.

RAD51AP1 expression in normal and breast tumor tissues and cell lines. A, *RAD51AP1* gene transcript levels were analyzed by semi-quantitative RT-PCR in human breast tumor tissues (T), both luminal ER$^+$ BC (n=5) and basal TNBC (n=6), and respective normal (N) tissues. B, Real-time RT-PCR (qPCR) analysis showing the relative mRNA expression of *RAD51AP1* in human normal and breast tumor tissues. C, TCGA database analysis confirms that increased *RAD51AP1* expression in human luminal ER$^+$ BC (n=358) and basal TNBC (n=98) when compared to normal (n=114). D, Kaplan-Meier Plots of relapse-free survival (RFS) of breast cancer patients in whole data sets for luminal ER$^+$ BC and basal TNBC stratified by RAD51AP1 expression. The P-value was calculated using long rank test. E and F, Semi-quantitative and qPCR analyses shows that increased *RAD51AP1* gene transcript levels in human luminal ER$^+$ BC (n=7), basal TNBC (n=4) cell lines when compared to non-transformed normal mammary epithelial (n=4).

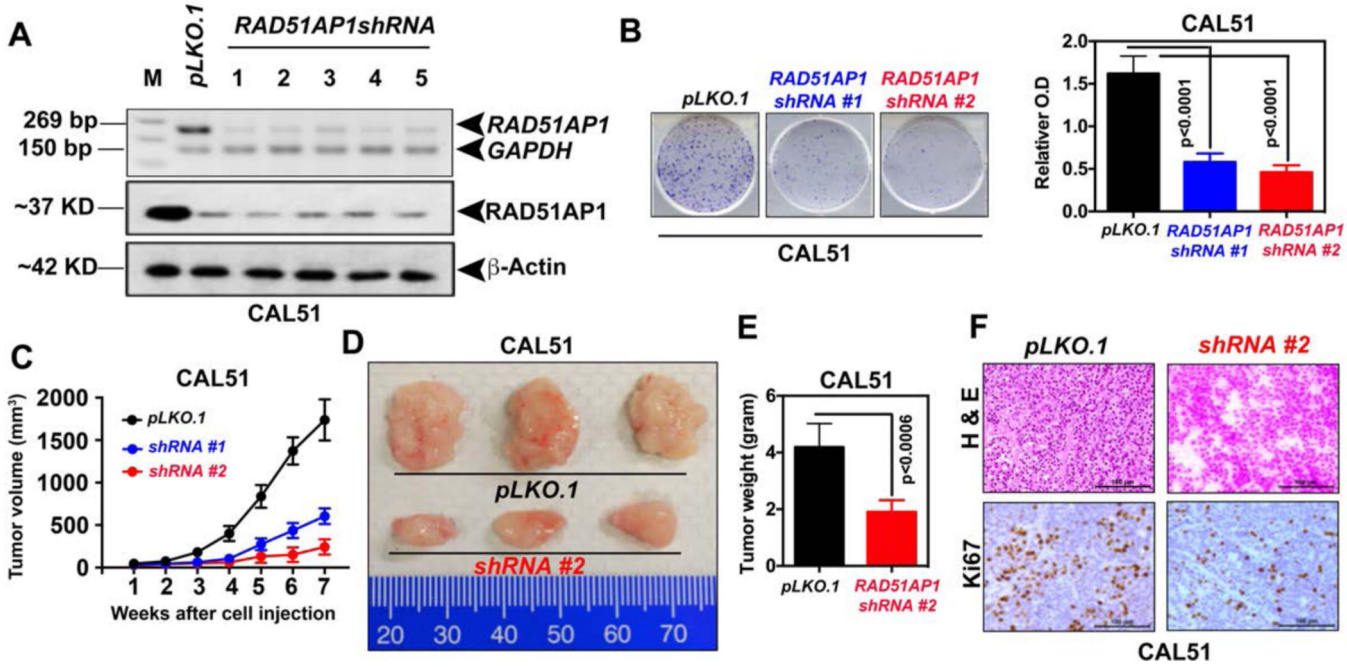

Figure 2.

RAD51AP1 KD in human breast cancer cells reduce tumor growth. A, *RAD51AP1* KD in CAL51 cell line was confirmed by semi-quantitative RT-PCR and western blot analyses. B, Representative images of colony-formation assay of CAL51-*pLKO.1* and CAL51-*RAD51AP1shRNA* (#1, and #2) stable cell lines show that *RAD51AP1* KD significantly reduces colony formation. The resulting colonies were stained with Giemsa dye following which, the bound Giemsa dye was dissolved and quantified by spectrophotometer analysis. Data represents mean ± SD from three independent experiments. C, Tumor growth measurement in mouse xenograft derived from CAL51-*pLKO.1* and CAL51-*RAD51AP1shRNA* (#1, and #2) shows that *RAD51AP1* KD significantly reduces tumor growth. (n=10 mice in each group). D, Representative images of mammary tumors tissues derived from CAL51-*pLKO.1* and CAL51-*RAD51AP1shRNA* (#2) mouse xenograft. (n=10 mice in each group). E, Tumor weight measurement shows that *RAD51AP1* KD significantly reduces tumor weight (grams). (n=10 mice in each group). **F** Hematoxylin and eosin (H & E)- and Ki67-stained images of tumor tissues derived from CAL51-*pLKO.1* and CAL51-*RAD51AP1shRNA* (#2) show a significantly reduced tumor burden in *RAD51AP1* KD cell lines by inhibition of tumor cell proliferation. Images were taken at 40x, scale bar represents 100 μm. (n=10 mice in each group).

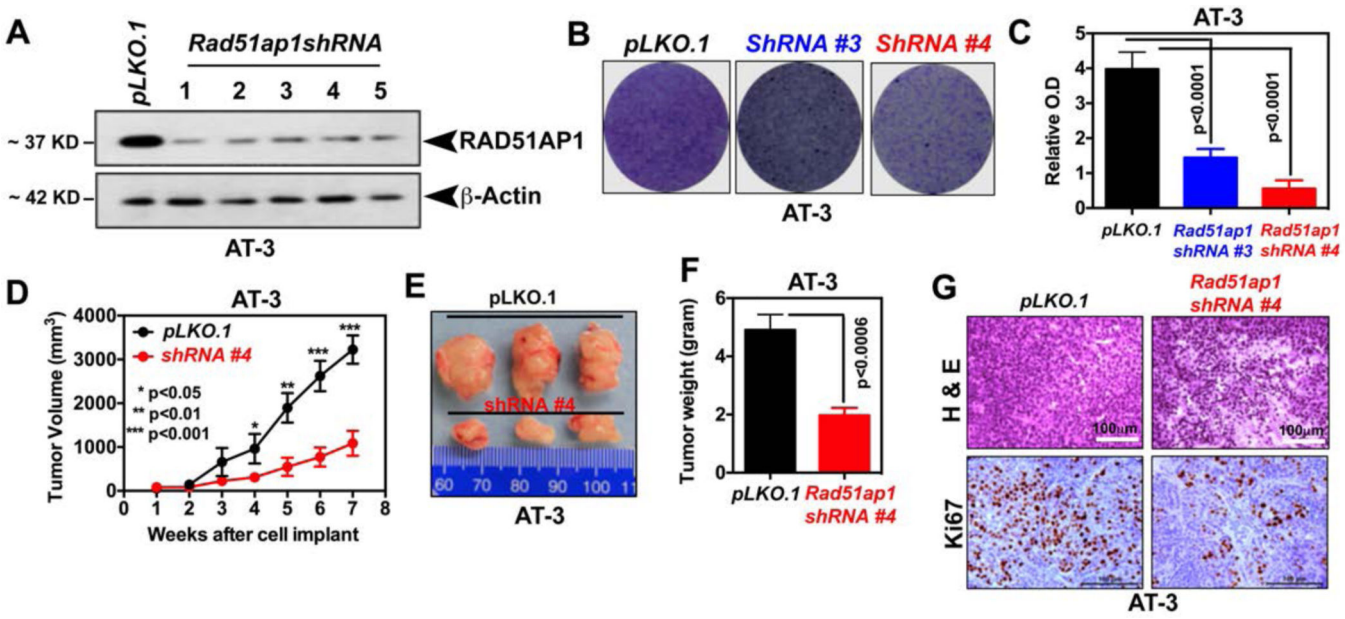

Figure 3.

Rad51ap1 KD reduced tumor growth in syngeneic mouse model. A, *Rad51ap1* KD in AT-3 cell line was confirmed by western blot analysis. (n=3 replicates). B and C, Representative images of colony-formation assay of AT-3-*pLKO.1* and AT-3-*Rad51ap1shRNA* (#3, and #4) stable cell lines show that *Rad51ap1* KD significantly reduces colony formation. The resulting colonies were stained with Giemsa dye and bound Giemsa dye were dissolved and quantified by spectrophotometer analysis. Data represents mean ± SD from three independent experiments. D, Tumor growth measurement in mouse syngeneic transplant from AT-3-*pLKO.1* and AT-3-*Rad51ap1shRNA* (#4) shows that *Rad51ap1* KD significantly reduces tumor growth. (n=10 mice in each group). E, Representative images of mammary tumors derived from AT-3-*pLKO.1* and AT-3-*Rad51ap1shRNA* (#4) mouse syngeneic transplant. (n=10 mice in each group). F, Tumor weight measurement shows that *Rad51ap1* KD significantly reduces tumor weight (grams). (n=10 mice in each group). G, Representative images of H & E and Ki67 staining of *pLKO.1* and *Rad51ap1shRNA* (#4) paraffin-embedded tumor sections show that *Rad51ap1* KD significantly reduced tumor burden by inhibiting cell proliferation. Images are taken at 60x, scale bar represents 100 μm.

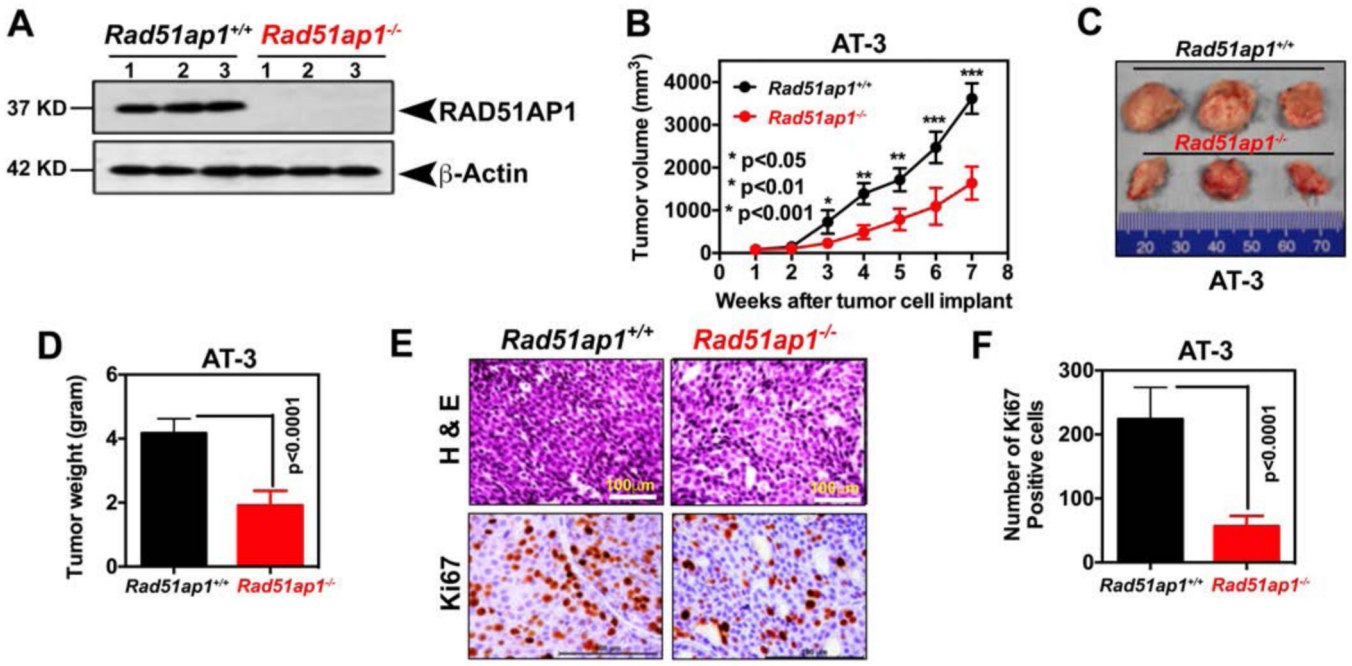

Figure 4.

Rad51ap1 knockout mice confer resistance to tumor growth. A, Representative western blot image of RAD51AP1 provided evidence that *Rad51ap1* knockout in mammary glands derived from wild-type (*Rad51ap1*$^{+/+}$) and Rad51ap1 knockout (*Rad51ap1*$^{-/-}$) mice. n=4 in each genotype. B, Tumor growth measurement in mouse syngeneic transplant derived from *Rad51ap1*$^{+/+}$ and *Rad51ap1*$^{-/-}$ mice show that *Rad51ap1* deficiency significantly reduced tumor growth. (n=10 mice in each group). Representative images of mammary tumors tissues C, and tumor weight (grams) D, driven by syngeneic transplant of AT-3 cell lines in *Rad51ap1*$^{+/+}$ and *Rad51ap1*$^{-/-}$ mice provide evidence that *Rad51ap1* deficiency significantly reduced tumor growth. (n=10 mice in each genotype). E, Representative images of H & E and Ki67 staining in tumor tissues of *Rad51ap1*$^{+/+}$ and *Rad51ap1*$^{-/-}$ mice provide evidence that *Rad51ap1* deletion significantly reduced tumor growth by inhibiting tumor cell proliferation. Images are taken at 60x, scale bar represents 100 μm. F, Total number of Ki67 positive cells analysis provide evidence that reduced Ki67 positive cell in *Rad51ap1*$^{-/-}$ mice when compared to *Rad51ap1*$^{+/+}$ mice.

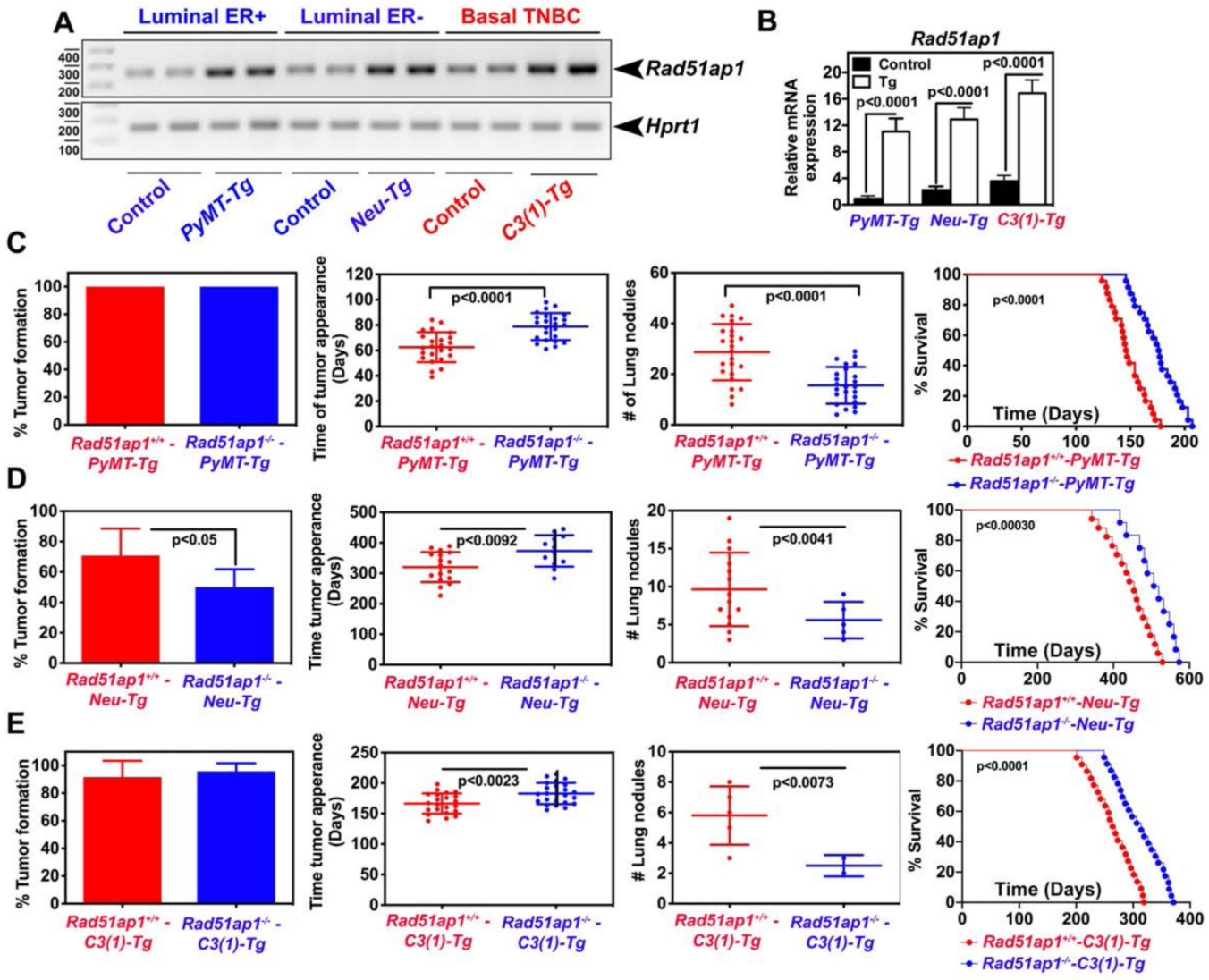

Figure 5.

Rad51ap1 deficiency impedes tumor growth in spontaneous mammary tumorigenesis. A, Representative image of semi-quantitative RT-PCR and B, qPCR analyses reveal that high *Rad51ap1* expression in tumor tissues derived from *PyMT-Tg*, *Neu-Tg*, and C3(1) -Tg mice. n=2 mice in each. C and E, although *Rad51ap1* deletion does not affect the overall tumor incidence in *PyMT-Tg* and *C3(1)-Tg* mice, it significantly delayed the time of tumor onset and the reduced number of lung nodules resulting in increased overall survival. n=24 mice in each genotype. D, *Rad51ap1* deficiency significantly reduced tumor incidence, time of tumor onset, and number of lung nodules in *Neu-Tg* mice with increased overall survival. (n=24 mice in each genotype).

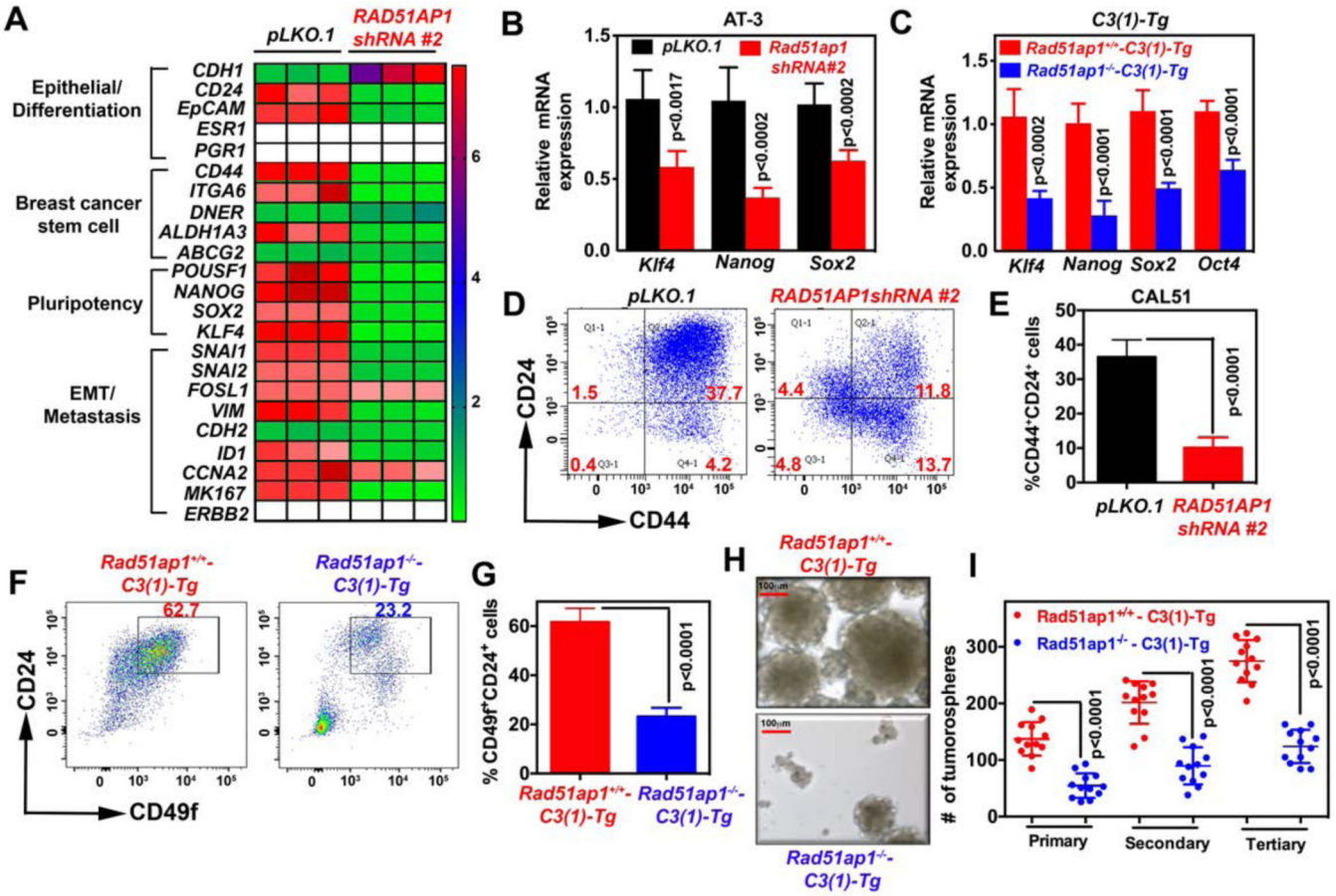

Figure 6.

RAD51AP1 KD reduces cancer stem cell self-renewal signaling. A, Heat map generated from the qPCR dataset for epithelial differentiation, breast cancer stem cell marker, pluripotency, and EMT/Metastasis of CAL51-*pLKO.1* and CAL51-*RAD51AP1*(#2) cells (n=3 independent clones with triplicates = 9 dataset in each). B, Relative expression of breast cancer stem cell self-renewal genes in AT-3-*pLKO.1* and AT-3-*Rad51ap1shRNA* (#3) by qPCR analysis. (n=3 independent clones with triplicates = 9 dataset in each). C, Relative expression of breast cancer stem cell self-renewal genes in *Rad51ap1*$^{+/+}$-*C3(1)-Tg* and *Rad51ap1*$^{-/-}$-*C3(1)-Tg* by qPCR analysis. (n=3 mice with triplicates =9 dataset in each). D and E, Representative FACS dot plots and quantification of BCSC (CD49f^{+}CD24^{+}) in CAL51-*pLKO.1* and CAL51-*RAD51AP1shRNA* (#2) cells. F and G, Representative FACS dot plots and quantification of BCSC in *Rad51ap1*$^{+/+}$-*C3(1)-Tg* and *Rad51ap1*$^{-/-}$-*C3(1)-Tg* mice. H and I, Representative images of tumorospheres generated form *Rad51ap1*$^{+/+}$-*C3(1)-Tg* and *Rad51ap1*$^{-/-}$-*C3(1)-Tg* mice and quantification of primary, secondary, and tertiary tumorospheres number (n=3–5 mice in each).

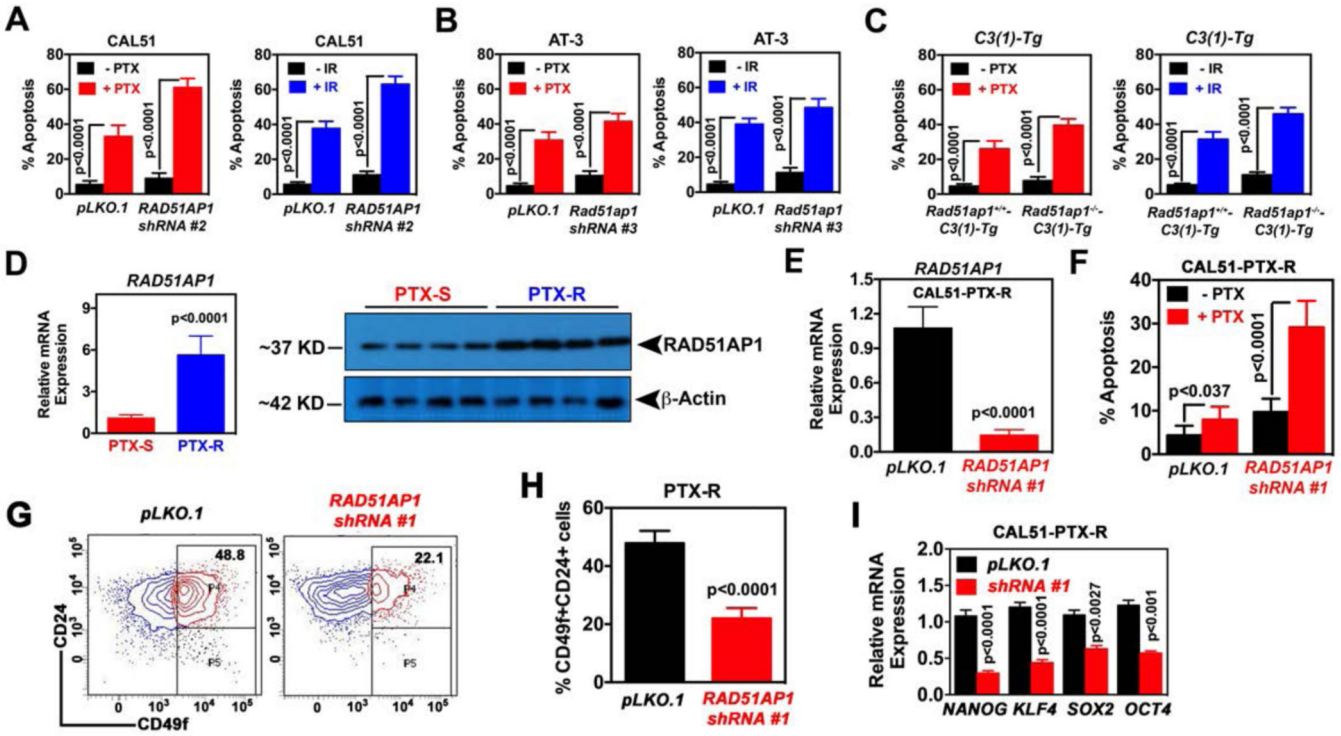

Figure 7.

RAD51AP1 KD potentiates chemotherapy and radiation therapy response by inhibiting stem cell self-renewal signaling. A, Percent apoptosis (Annexin V^+/PI^-) was calculated in CAL51-*pLKO.1* and CAL51-*RAD51AP1shRNA* transfected cells with PTX (10 nM) and IR (10 Gy), respectively. B and C, Similarly, percent apoptosis was calculated in AT-3-*pLKO.1* and AT-3-*RAD51AP1shRNA* transfected cells as well as cell isolated from the mammary tumor tissues obtained from *Rad51ap1*$^{+/+}$-*C3(1)-Tg* and *Rad51ap1*$^{+/+}$-*C3(1)-Tg* mice with PTX (10 nM) and IR (10 Gy), respectively. Values are expressed as Mean ± SD of three independent experiments or three mice in each with triplicated values = 9 datasets. D, *RAD51AP1* mRNA and RAD51AP1 protein expression in PTX-S (sensitive) and PTX-R (resistant) CAL51 cell lines as measured by qPCR and western blot, respectively. n=4 independent clones. E, Relative *RAD51AP1* transcript expression in CAL51-PTX-R cells transfected with *pLKO.1* and *RAD51AP1shRNA*. F, percent apoptosis was calculated in PTX-R-*pLKO.1*- and PTX-R-*RAD51AP1shRNA*-transfected cells treated with and without PTX (10 nM for 48 h). G and H, Representative FACS contour plots and quantification of BCSC ($CD49f^+CD24^+$) in CAL51-PTX-R-*pLKO.1* and CAL51-PTX-R-*RAD51AP1shRNA* cells. I, Relative expression of stem cell self-renewal genes in CAL51-PTX-R-*pLKO.1* and CAL51-PTX-R-*RAD51AP1shRNA* cells.